ESC HEART FAILURE
ESC Heart Failure 2020; **7**: 2992–3002
Published online 25 July 2020 in Wiley Online Library (wileyonlinelibrary.com) **DOI:** 10.1002/ehf2.12918

ORIGINAL RESEARCH ARTICLE

Sacubitrilat reduces pro-arrhythmogenic sarcoplasmic reticulum Ca^{2+} leak in human ventricular cardiomyocytes of patients with end-stage heart failure

Jörg Eiringhaus[1,2,3], Christoph M. Wünsche[1,2], Petros Tirilomis[1,2], Jonas Herting[1,2], Nadja Bork[4], Viacheslav O. Nikolaev[4], Gerd Hasenfuss[1,2], Samuel Sossalla[1,2,5] and Thomas H. Fischer[1,2,6]*

[1]*Abt. Kardiologie und Pneumologie/Herzzentrum, Georg-August-Universität Göttingen, Göttingen, Germany;* [2]*Deutsches Zentrum für Herz-Kreislauf Forschung (DZHK), Standort Göttingen, Göttingen, Germany;* [3]*Abt. Kardiologie und Angiologie, Medizinische Hochschule Hannover, Hanover, Germany;* [4]*Institut für Experimentelle Herz-Kreislaufforschung, Universitätsklinikum Hamburg-Eppendorf, Hamburg, Germany;* [5]*Klinik und Poliklinik für Innere Medizin II, Universitätsklinikum Regensburg, Regensburg, Germany;* [6]*Abt. Kardiologie, Medizinische Klinik und Poliklinik I, Universitätsklinikum Würzburg, Oberdürrbacher Straße 6, Würzburg, 97080, Germany*

Abstract

Aims Inhibition of neprilysin and angiotensin II receptor by sacubitril/valsartan (Val) (LCZ696) reduces mortality in heart failure (HF) patients compared with sole inhibition of renin–angiotensin system. Beneficial effects of increased natriuretic peptide levels upon neprilysin inhibition have been proposed, whereas direct effects of sacubitrilat (Sac) (LBQ657) on myocardial Ca^{2+} cycling remain elusive.

Methods and results Confocal microscopy (Fluo-4 AM) was used to investigate pro-arrhythmogenic sarcoplasmic reticulum (SR) Ca^{2+} leak in freshly isolated murine and human ventricular cardiomyocytes (CMs) upon Sac (40 μmol/L)/Val (13 μmol/L) treatment. The concentrations of Sac and Val equalled plasma concentrations of LCZ696 treatment used in PARADIGM-HF trial. Epifluorescence microscopy measurements (Fura-2 AM) were performed to investigate effects on systolic Ca^{2+} release, SR Ca^{2+} load, and Ca^{2+}-transient kinetics in freshly isolated murine ventricular CMs. The impact of Sac on myocardial contractility was evaluated using *in toto*-isolated, isometrically twitching ventricular trabeculae from human hearts with end-stage HF. Under basal conditions, the combination of Sac/Val did not influence diastolic Ca^{2+}-spark frequency (CaSpF) nor pro-arrhythmogenic SR Ca^{2} leak in isolated murine ventricular CMs (n CMs/hearts = 80/7 vs. 100/7, P = 0.91/0.99). In contrast, Sac/Val treatment reduced CaSpF by 35 ± 9% and SR Ca^{2+} leak by 45 ± 9% in CMs put under catecholaminergic stress (isoproterenol 30 nmol/L, n = 81/7 vs. 62/7, $P < 0.001$ each). This could be attributed to Sac, as sole Sac treatment also reduced both parameters by similar degrees (reduction of CaSpF by 57 ± 7% and SR Ca^{2+} leak by 76 ± 5%; n = 101/4 vs. 108/4, $P < 0.01$ each), whereas sole Val treatment did not. Systolic Ca^{2+} release, SR Ca^{2+} load, and Ca^{2+}-transient kinetics including SERCA activity (k_{SERCA}) were not compromised by Sac in isolated murine CMs (n = 41/6 vs. 39/6). Importantly, the combination of Sac/Val and Sac alone also reduced diastolic CaSpF and SR Ca^{2+} leak (reduction by 74 ± 7%) in human left ventricular CMs from patients with end-stage HF (n = 71/8 vs. 78/8, $P < 0.05$ each). Myocardial contractility of human ventricular trabeculae was not acutely affected by Sac treatment as the developed force remained unchanged over a time course of 30 min (n trabeculae/hearts = 3/3 vs. 4/3).

Conclusion This study demonstrates that neprilysin inhibitor Sac directly improves Ca^{2+} homeostasis in human end-stage HF by reducing pro-arrhythmogenic SR Ca^{2+} leak without acutely affecting systolic Ca^{2+} release and inotropy. These effects might contribute to the mortality benefits observed in the PARADIGM-HF trial.

Keywords Heart failure; Entresto; Neprilysin inhibition; Ca cycling; SR Ca leak; Arrhythmia

Received: 4 September 2019; Revised: 20 May 2020; Accepted: 13 July 2020
**Correspondence to: Thomas H. Fischer, Abt. Kardiologie, Medizinische Klinik und Poliklinik I, Universitätsklinikum Würzburg, Oberdürrbacher Straße 6, 97080 Würzburg, Germany. Email: fischer_t@ukw.de*

Introduction

Pharmacological inhibition of neurohumoral pathways, such as the renin–angiotensin–aldosterone system (RAAS), has become a central point in the treatment of heart failure (HF) during the last decades.[1] Ever since, there has also been interest in the potential benefit of an augmentation of endogenous natriuretic peptides (NPs) as they have diuretic, natriuretic and vasodilating effects and are able to inhibit RAAS and pathological growth (e.g. hypertrophy and fibrosis) in HF.[2] As an administration of exogenous NPs failed to improve cardiovascular outcome,[3] great efforts have been made to inhibit the NP-degrading enzyme neprilysin that acts as a membrane-bound neutral endopeptidase and can be found mainly in the kidney, myocardium, and vascular endothelium.[4] The pivotal PARADIGM-HF trial could demonstrate that simultaneous blockage of neprilysin (sacubitril) and angiotensin II receptors [valsartan (Val)] by LCZ696 resulted in a 20% reduction of cardiovascular death and a 16% reduction of all-cause mortality in patients with HF with reduced ejection fraction (HFrEF) compared with enalapril (sole angiotensin-converting enzyme inhibition).[5] Conclusively, the combined angiotensin receptor/neprilysin inhibitor (ARNI) LCZ696 was implemented into the current European Society of Cardiology guidelines for HF therapy.[6] On the molecular level, the NPs atrial natriuretic peptide (ANP) and brain natriuretic peptide (BNP) exert their physiological function via binding to the NP receptors type A and type B and consecutive activation of cyclic guanosine monophosphate-dependent pathways.[7] In line with this, neprilysin inhibition was shown to result in an increase of plasma and urinary cyclic guanosine monophosphate levels and urinary atrial natriuretic peptide levels in HFrEF patients.[8] Therefore, mortality and morbidity reduction upon neprilysin inhibition is currently mainly attributed to beneficial circulatory effects of increased NP levels. Interestingly, it has recently been reported that ARNI treatment also decreased ventricular arrhythmias and appropriate implantable cardioverter defibrillator (ICD) shocks in HFrEF patients with implantable cardiac devices compared with sole angiotensin inhibition. Thus, an antiarrhythmic effect of this treatment has been claimed.[9] Nevertheless, it is still unclear if this effect is indirectly caused by systemic circulatory effects or by direct beneficial antiarrhythmic effects of neprilysin inhibition on cardiomyocytes (CMs), which could be of interest for the development of further therapeutics. Therefore, this study is the first that aims at elucidating the effects of neprilysin inhibition on ventricular Ca^{2+} cycling and arrhythmogenic activity in murine and human CMs.

Methods

Myocyte isolation of murine ventricular cardiomyocytes

Isolation of murine ventricular CMs from wild-type (WT) mice (B6N) was performed as reported in previous publications of our group.[10,11] A Langendorff apparatus was used to retrogradely perfuse the explanted hearts with an initially Ca^{2+}-free Tyrode's solution containing (in mmol/L) NaCl 113, KCl 4.7, KH_2PO_4 0.6, $Na_2HPO_4{\cdot}2H_2O$ 0.6, $MgSO_4{\cdot}7H_2O$ 1.2, $NaHCO_3$ 12, $KHCO_3$ 10, HEPES 10, taurine 30, BDM 10, glucose 5.5, and phenol red 0.032 (37°C, pH 7.4). Then, 7.5 mg/mL of Liberase 1 (Roche Diagnostics, Mannheim, Germany), trypsin 0.6% (Life Technologies, Carlsbad, CA, USA), and 0.125 mmol/L of $CaCl_2$ were added to the perfusion solution. Once the tissue became flaccid, atrial and ventricular myocardium was separated by cutting off the ventricles beneath the atrioventricular valve level. The ventricular myocardium was cut into small pieces and, again, dispersed in Tyrode's solution. Concentration of Ca^{2+} was stepwise increased every 3 min until target concentration was reached (2 mmol/L). Cells were plated on laminin-coated recording chambers and left for 15 min to enable settling.

Human myocardial tissue acquisition and myocyte isolation

All procedures with respect to human myocardial tissue were conducted in compliance with the local ethics committee, and written informed consent was received from all participants prior to inclusion. In our study, left ventricular myocardial tissue was taken from explanted hearts of 11 patients with end-stage HF (New York Heart Association Heart Failure Classification IV). Detailed patient characteristics are annotated in *Tables 1* and *2*. As reported previously, the explanted hearts were directly acquired in the operating room during surgical procedure and immediately put in pre-cooled cardioprotective solution (Custodiol®, Dr. Franz Köhler Chemie, Bensheim, Germany; in mmol/L: NaCl 15, KCl 9, $MgCl_2$ 4, histidine hydrochloride monohydrate 18, histidine 180, tryptophan 2, mannitol 30, $CaCl_2$ 0.015, and potassium hydrogen 2-oxopentandiate 1).[12,13] Afterwards, heart tissue used for cell isolation of left ventricular CMs was resected as described before.[12,14] Human myocardium was rinsed, cut into small pieces, and incubated at 37°C in a spinner flask filled with Joklik-MEM solution (JMEM, pH 7.4, 37°C; AppliChem, Darmstadt, Germany) containing 1.0 mg/mL of collagenase (Worthington type 2, 250 U/mg) and trypsin (2.5 g/L; Life Technologies). After 45 min, the supernatant was discarded, and fresh JMEM solution containing only collagenase was added. The solution was incubated for 10 min until myocytes were disaggregated using a Pasteur pipette. The supernatant containing disaggregated cells was removed and centrifuged (500 r.p.m., 22 g, 5 min). Fresh JMEM with collagenase was added to the remaining tissue. This procedure was repeated 4–5 times. After every step, the centrifuged cells were resuspended in JMEM solution containing 10% bovine calf serum (pH 7.4, KOH, room temperature).

Table 1 Characteristics of patients whose myocardial tissue was used for confocal microscopy measurements

	Human HF (n = 8)
Male sex (%)	75.0
Age (mean ± SEM, years)	51.8 ± 3.7
Ejection fraction (mean ± SEM, %)	31.3 ± 3.2
Ischaemic heart disease (%)	37.5
Diabetes (%)	25.0
ACE inhibitors (%)	57.1
Beta-blockers (%)	100
Diuretics (%)	86.0
Digoxin (%)	14.0
Amiodaron (%)	14.0
AT_1 receptor antagonists (%)	0.0
Aldosterone antagonists (%)	71.0
PDE inhibitors (%)	29.0
Ca^{2+}-channel blockers (%)	0.0

ACE, angiotensin-converting enzyme; AT_1, angiotensin II receptor type 1; HF, heart failure; PDE, phosphodiesterase; SEM, standard error of the mean.
Annotation in mean ± SEM or %, respectively.

Table 2 Characteristics of patients whose myocardial tissue was used for muscle twitch experiments

	Human HF (n = 3)
Male sex (%)	66.7
Age (mean ± SEM, years)	55 ± 4
Ejection fraction (mean ± SEM, %)	11 ± 6.4
Ischaemic heart disease (%)	0
Diabetes (%)	0
ACE inhibitors (%)	0
Beta-blockers (%)	100
Diuretics (%)	100
Digoxin (%)	0
Amiodaron (%)	33.3
AT_1 receptor antagonists (%)	0
Aldosterone antagonists (%)	66.7
PDE inhibitors (%)	0
Ca^{2+}-channel blockers (%)	0

ACE, angiotensin-converting enzyme; AT_1, angiotensin II receptor type 1; HF, heart failure; PDE, phosphodiesterase; SEM, standard error of the mean.
Annotation in mean ± SEM or %, respectively.

Only cell solutions containing elongated, not granulated CMs with cross-striations were selected for experiments, plated on laminin-coated recording chambers, and left to settle for 30 min.

Intracellular Ca^{2+} imaging

Confocal microscopy

Isolated CMs were incubated at room temperature for 15 min (murine CMs)/30 min (human CMs) with a Fluo-4 AM loading buffer (10 μmol/L each; Molecular Probes, Eugene, OR, USA), which contained no active agent (control group), LBQ657 [sacubitrilat (Sac) 40 μmol/L; AOBIOUS, Gloucester, MA, USA], Val (13 μmol/L; Sigma-Aldrich, Steinheim, Germany), or combination of Sac and Val (Sac/Val). Concentrations of Sac and Val were chosen according to the plasma concentrations measured under LCZ696 treatment (200 mg twice daily) in the course of a pharmacokinetic study aiming at elucidating respective plasma concentrations in the PARADIGM-HF trial.[5,8] To ensure proper effect of neprilysin inhibition, the active moiety Sac (LBQ657), which results upon metabolization of the prodrug sacubitril (AHU377) via enzymatic cleavage of its ethyl ester group, was used for *in vitro* experiments in our study.[15] To increase basal sarcoplasmic reticulum (SR) Ca^{2+} leak in experiments on murine WT CMs, 30 nmol/L of isoproterenol (Iso) was additionally added.

Experimental solution contained (mmol/L): KCl 4, NaCl 140, $MgCl_2$ 1, HEPES 5, glucose 10, $CaCl_2$ 1 (human)/2 (murine), and the respective active agents (pH 7.4, NaOH, room temperature). To wash out the loading buffer and remove any extracellular dye as well as to allow enough time for complete de-esterification of the fluorescent dye, cells were superfused with experimental solution for 5 min before experiments were started. Cells were continuously superfused during experiments. Ca^{2+}-spark measurements were performed with a laser scanning confocal microscope (LSM 5 Pascal, Zeiss, Jena, Germany) using a 40× oil immersion objective. Fluo-4 was excited by an argon ion laser (488 nm), and emitted fluorescence was collected through a 505 nm long-pass emission filter. Fluorescence images were recorded in the line-scan mode with 512 pixels per line (width of each scanline: 38.4 μm) and a pixel time of 0.64 μs. One image consists of 10 000 unidirectional line scans, equating to a measurement period of 7.68 s. Experiments were conducted at resting conditions after loading the SR with Ca^{2+} by repetitive field stimulation (30 beats at 3 Hz for murine CMs and 10 beats at 1 Hz for human CMs; 20 V each). The Ca^{2+}-spark frequency (CaSpF) and dimensions of each CM were analysed with the program SparkMaster for ImageJ.[16] The mean spark frequency of the respective cell (CaSpF) resulted from the number of sparks normalized to cell width and scan rate (100 μm/s). Ca^{2+}-spark size was calculated as the product of spark amplitude (F/F_0), duration, and width. The average leak per cell was inferred by multiplying Ca^{2+}-spark size by CaSpF.

Epifluorescence microscopy

Cardiomyocytes were isolated and plated as described earlier and incubated with a Fura-2 AM loading buffer (10 μmol/L; Molecular Probes) for 15 min (murine CMs). In the intervention groups, the loading buffer also contained the respective active agents as described earlier for confocal microscopic measurements. After staining, the CMs were incubated with experimental solution for 15 min before measurements were started to enable complete de-esterification of intracellular Fura-2. During measurements, CMs were continuously superfused with experimental solution. Measurements were performed with a Motic AE32 microscope (Speed Fair Co.,

Ltd., Hong Kong) provided with a fluorescence detection system (IonOptix Corp., Milton, MA, USA). Cells were excited at 340 and 380 nm, and the emitted fluorescence was collected at 510 nm. The intracellular Ca^{2+} level was measured as the ratio of fluorescence at 340 and 380 nm ($F_{340\ nm}/F_{380\ nm}$ in ratio units). Systolic Ca^{2+} transients were recorded at steady-state conditions under constant field stimulation (1 and 3 Hz). To assess the SR Ca^{2+} content, we measured the amplitude of caffeine-induced Ca^{2+} transients. After stopping the stimulation during steady-state conditions at 1 Hz, caffeine (10 mmol/L; Sigma-Aldrich) was applied directly onto the cell leading to immediate and complete SR Ca^{2+} release. The recorded Ca^{2+} transients were analysed with the software IonWizard® (IonOptix Corp.).

Myocardial contractility measurements (human muscle twitches)

To assess the effects of LBQ657 (Sac, 40 μmol/L) on the contractility of human HF myocardium, we performed experiments with *in toto*-isolated isometrically twitching ventricular trabeculae from human hearts (Con vs. Sac; one/two trabeculae per group per heart) explanted from patients with end-stage HF. Detailed patient characteristics are annotated in *Table 2*. Tissue was stimulated with 1 Hz over a time course of 30 min. Contractility experiments were performed as previously reported.[17]

Statistics

All data are presented as mean ± standard error of the mean. One-way ANOVA with Tukey's *post hoc* test (*Figures 1–4*) or two-way ANOVA with Sidak's *post hoc* test (*Figure 5*) was used to perform multiple comparison tests. Values of $P < 0.05$ were considered as statistically significant.

Results

Effects of combined angiotensin receptor and neprilysin inhibition on sarcoplasmic reticulum Ca^{2+} leak in murine wild-type cardiomyocytes

The impact of combined angiotensin receptor and neprilysin inhibition by Sac (40 μmol/L) and Val (13 μmol/L) on SR Ca^{2+} leak in isolated murine WT ventricular CMs was investigated by confocal microscopy (Fluo-4 AM). As annotated, Iso (30 nmol/L) was used in some groups for additional catecholaminergic stimulation.

In murine ventricular WT CMs and under basal conditions, ARNI treatment did not result in significant alterations of CaSpF (Sac + Val vs. Con: 0.31 ± 0.06 vs. 0.38 ± 0.07 × 100 μm/s, *n* cells/hearts = 100/7 vs. 80/7, $P = 0.91$, *Figure 1B*), Ca^{2+}-spark amplitude (F/F_0: 1.76 ± 0.03 vs. 1.70 ± 0.03, $P = 0.83$, *Figure 1C*), width (2.90 ± 0.12 vs. 2.62 ± 0.13 μm, $P = 0.66$, *Figure 1D*), and duration compared

Figure 1 Effects of combined angiotensin receptor and neprilysin inhibition [sacubitrilat (Sac) 40 μmol/L + valsartan (Val) 13 μmol/L] on diastolic sarcoplasmic reticulum (SR) Ca^{2+} leak in murine wild-type cardiomyocytes with and without β-adrenergic stimulation with isoproterenol (Iso, 30 nmol/L). (A) Representative confocal line scans of murine ventricular cardiomyocytes and respective quantification of (B) Ca^{2+}-spark frequency (CaSpF) as well as (C) amplitude, (D) width, and (E) duration of detected Ca^{2+} sparks and (F) total calculated SR Ca^{2+} leak normalized to control (Con). *Significant vs. Con; #significant vs. Iso ($P < 0.05$).

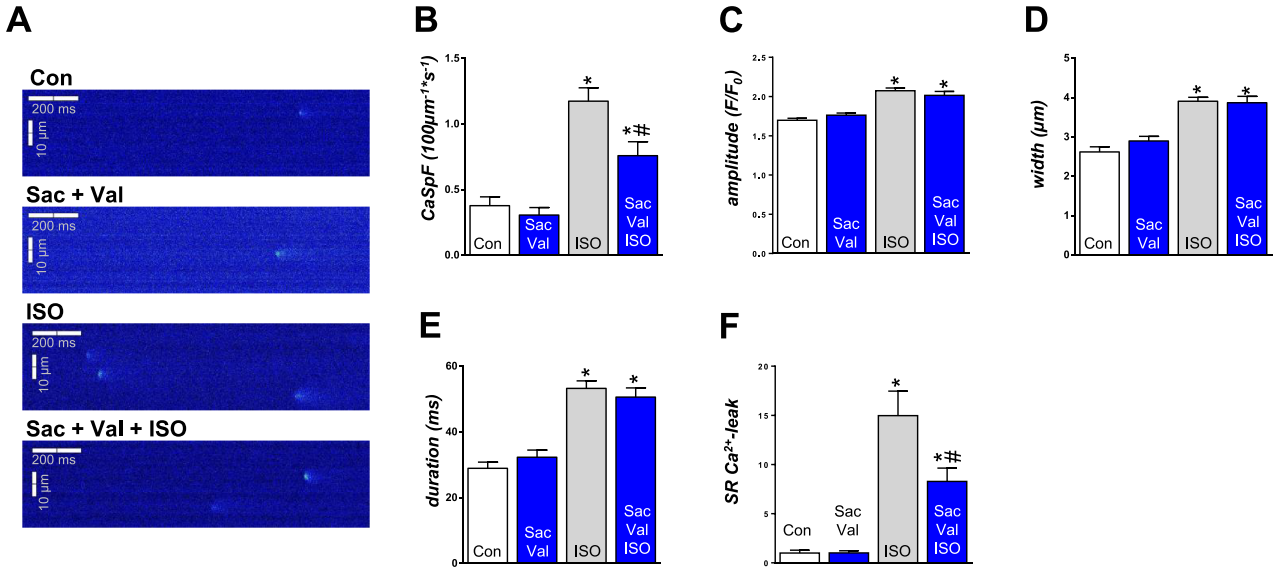

Figure 2 Effects of sole angiotensin receptor or neprilysin inhibition [sacubitrilat (Sac) 40 μmol/L + valsartan (Val) 13 μmol/L] on diastolic sarcoplasmic reticulum (SR) Ca^{2+} leak in murine wild-type cardiomyocytes upon β-adrenergic stimulation with isoproterenol (Iso, 30 nmol/L). (A) Representative confocal line scans of murine ventricular cardiomyocytes and respective quantification of (B) Ca^{2+}-spark frequency (CaSpF) as well as (C) amplitude, (D) width, and (E) duration of detected Ca^{2+} sparks and (F) total calculated SR Ca^{2+} leak normalized to control (Con). *Significant vs. Con; #significant vs. Iso ($P < 0.05$).

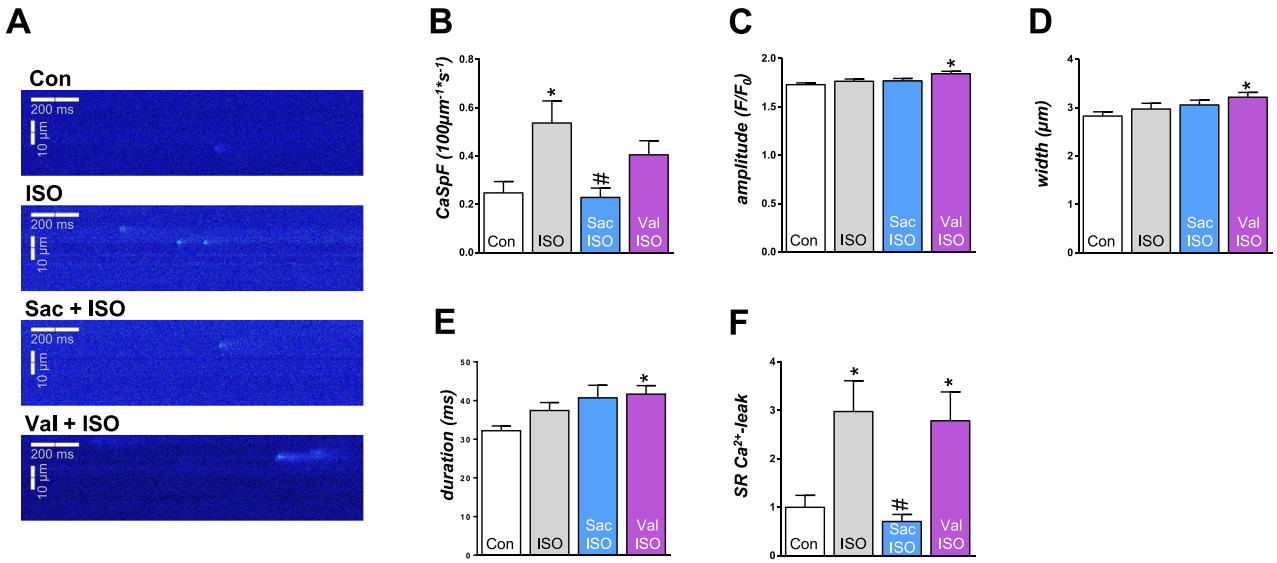

with untreated control (32.31 ± 2.18 vs. 28.94 ± 1.88 ms, $P = 0.90$, *Figure 1E*). In line with this, the calculated SR Ca^{2+} leak was also not significantly altered ($P = 0.99$, *Figure 1F*). As expected, β-adrenergic stimulation using Iso resulted in a significant increase of CaSpF (Iso vs. Con, *n* cells/hearts = 81/7 vs. 80/7: 1.18 ± 0.10 vs. 0.38 ± 0.07 × 100 μm/s, $P < 0.0001$, *Figure 1B*), amplitude (F/F_0: 2.08 ± 0.04 vs. 1.70 ± 0.03, $P < 0.0001$, *Figure 1C*), width (3.91 ± 0.10 vs. 2.62 ± 0.13 μm, $P < 0.0001$, *Figure 1D*), and duration (53.26 ± 2.29 vs. 28.94 ± 1.88 ms, $P < 0.0001$, *Figure 1E*), which translated into a significantly increased SR Ca^{2+} leak compared with untreated control (~15-fold increase, $P < 0.0001$, *Figure 1F*). Interestingly, in the setting of β-adrenergic stimulation, ARNI treatment yielded a significant reduction of CaSpF (Sac + Val + Iso vs. Iso, *n* cells/hearts = 62/7 vs. 81/7: 0.76 ± 0.11 vs. 1.18 ± 0.10 × 100 μm/s, $P < 0.01$, *Figure 1B*) as well as calculated SR Ca^{2+} leak (decrease by 45 ± 9%, $P < 0.01$, *Figure 1F*), whereas Ca^{2+}-spark amplitude (F/F_0: 2.02 ± 0.05 vs. 2.08 ± 0.04, $P = 0.67$, *Figure 1C*), width (3.87 ± 0.16 vs. 3.91 ± 0.10 μm, $P = 0.99$, *Figure 1D*), and duration (50.62 ± 2.80 vs. 53.26 ± 2.29 ms, $P = 0.86$, *Figure 1E*) remained unchanged compared with sole Iso treatment. In other words, the steep increase of pro-arrhythmogenic SR Ca^{2+} leak in murine ventricular CMs induced by Iso (~15-fold) could be reduced to nearly 50% upon ARNI treatment (*Figure 1F*).

Effects of sole angiotensin receptor or neprilysin inhibition on sarcoplasmic reticulum Ca^{2+} leak in murine wild-type cardiomyocytes

To elucidate which of the two components was responsible for the reductions of CaSpF and SR Ca^{2+} leak upon ARNI treatment under β-adrenergic stimulation (*Figure 1*), we performed further experiments on murine WT CMs in which angiotensin receptor inhibition (Val, 13 μmol/L) and neprilysin inhibition (Sac, 40 μmol/L) were executed separately (*Figure 2*). Again, Iso (30 nmol/L) was used for catecholaminergic stimulation.

As shown before, β-adrenergic stimulation with Iso led to a significant increase of CaSpF (Iso vs. Con: 0.54 ± 0.09 vs. 0.25 ± 0.05 × 100 μm/s, *n* cells/hearts = 101/4 vs. 120/4, $P < 0.01$, *Figure 2B*) and SR Ca^{2+} leak compared with untreated control (~3-fold increase, $P = 0.01$, *Figure 2F*). Indeed, additional neprilysin inhibition by Sac yielded a significant reduction of CaSpF (Sac + Iso vs. Iso: 0.23 ± 0.04 vs. 0.54 ± 0.09 × 100 μm/s, *n* cells/hearts = 108/4 vs. 101/4, $P < 0.01$, *Figure 2B*) as well as calculated SR Ca^{2+} leak (decrease by 76 ± 5%, $P < 0.01$, *Figure 2F*), whereas Ca^{2+}-spark amplitude (F/F_0: 1.77 ± 0.03 vs. 1.77 ± 0.02, $P = 0.99$, *Figure 2C*), width (3.06 ± 0.10 vs. 2.97 ± 0.12 μm, $P = 0.95$, *Figure 2D*), and duration (40.68 ± 3.28 vs. 37.45 ± 2.04 ms, $P = 0.78$, *Figure 2E*) were not affected compared with sole Iso treatment. Sole angiotensin receptor inhibition by Val,

Figure 3 Effects of neprilysin inhibition [sacubitrilat (Sac) 40 μmol/L and isoproterenol (Iso) 30 nmol/L] on calcium-cycling properties of murine ventricular cardiomyocytes. (A) Representative original recordings of systolic (1 and 3 Hz) and caffeine-induced Ca^{2+} transients (arrow indicates caffeine application) as well as respective quantification of (B) systolic Ca^{2+}-transient amplitude at 1 Hz and (C) 3 Hz stimulation. (D) Amplitude (peak *h*) of caffeine-induced Ca^{2+} transients. (E) Decay kinetics (RT_{50}) of systolic Ca^{2+} transients at 1 Hz and (F) 3 Hz. (G) SERCA activity (k_{SERCA}). *Significant vs. Con; #significant vs. Iso ($P < 0.05$). Con, control.

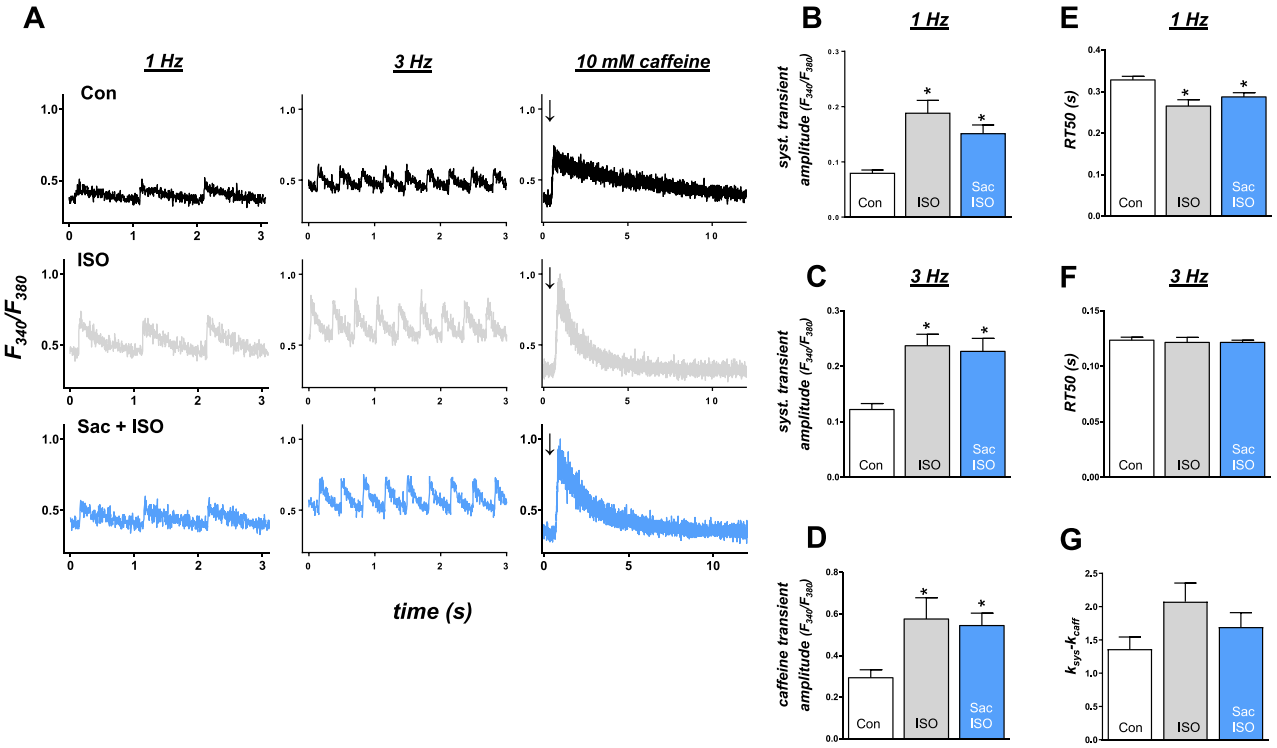

Figure 4 Effects of angiotensin receptor and neprilysin inhibition [sacubitrilat (Sac) 40 μmol/L/Sac + valsartan (Val) 13 μmol/L] on diastolic sarcoplasmic reticulum (SR) Ca^{2+} leak in human cardiomyocytes of patients with end-stage heart failure. (A) Representative confocal line scans of murine ventricular cardiomyocytes and respective quantification of (B) Ca^{2+}-spark frequency (CaSpF) as well as (C) amplitude, (D) width, and (E) duration of detected Ca^{2+}-sparks and (F) total calculated SR Ca^{2+} leak normalized to control (Con). *Significant vs. Con ($P < 0.05$).

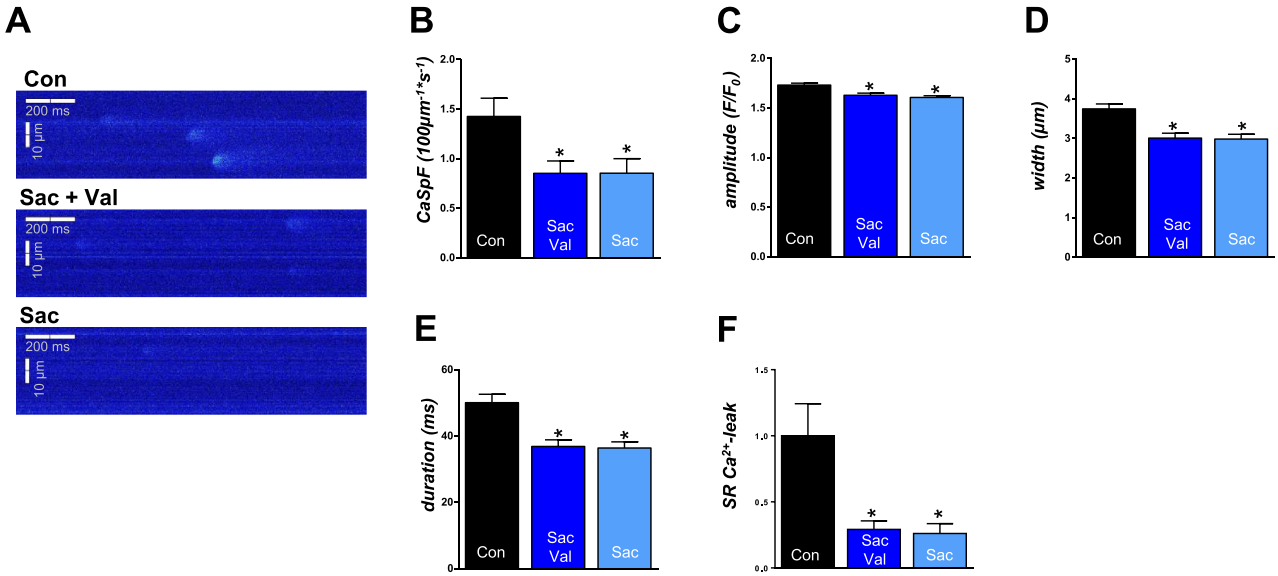

DOI: 10.1002/ehf2.12918

Figure 5 Effects of neprilysin inhibition [sacubitrilat (Sac) 40 μmol/L] on contractility of isometrically twitching ventricular trabeculae from human hearts of patients with end-stage heart failure. (A) Original twitches of isolated trabeculae and respective developed force of control (Con) and (B) Sac treatment. (C) Developed force normalized to Con (Tdev norm.) in time course of 30 min.

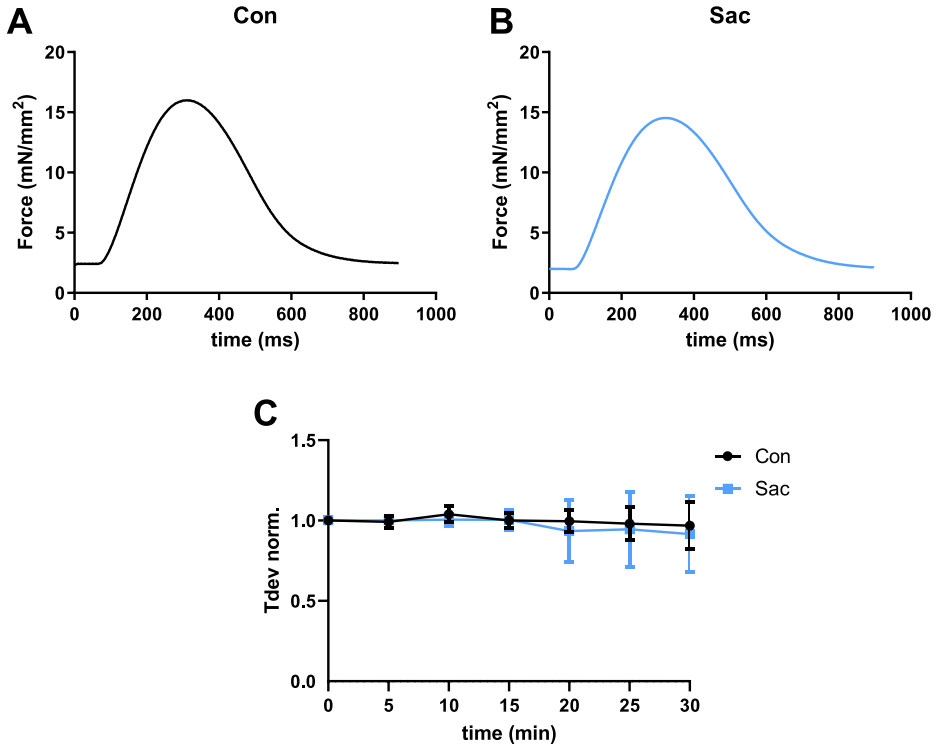

however, did not lead to significant alterations of CaSpF (Val + Iso vs. Iso: 0.40 ± 0.06 vs. 0.54 ± 0.09 × 100 μm/s, *n* cells/hearts = 117/4 vs. 101/4, *P* = 0.42, *Figure 2B*), Ca^{2+}-spark amplitude (F/F_0: 1.84 ± 0.03 vs. 1.77 ± 0.02, *P* = 0.08, *Figure 2C*), width (3.22 ± 0.10 vs. 2.97 ± 0.12 μm, *P* = 0.29, *Figure 2D*), and duration compared with sole Iso treatment (41.66 ± 2.21 vs. 37.45 ± 2.04 ms, *P* = 0.50, *Figure 2E*). In line with this, the SR Ca^{2+} leak was equal in both groups (*P* = 0.99, *Figure 2F*).

Effects of neprilysin inhibition on systolic Ca^{2+} release, sarcoplasmic reticulum Ca^{2+} load and Ca^{2+} reuptake in murine wild-type cardiomyocytes

As differences in the SR Ca^{2+} leak may also be attributed to altered SR Ca^{2+} loading, the influence of neprilysin inhibition on systolic Ca^{2+} release and SR Ca^{2+} content was analysed by epifluorescence microscopy (Fura-2 AM). Murine WT ventricular CMs were stimulated at 1 and 3 Hz to record systolic Ca^{2+} transients, and caffeine application was used to quantify SR Ca^{2+} content (*Figure 3A*). Systolic Ca^{2+}-transient amplitude was significantly increased upon Iso treatment under stimulation with 1 Hz (Iso vs. Con: F_{340}/F_{380}: 0.19 ± 0.02 vs. 0.08 ± 0.01, *n* cells/hearts = 41/6 vs. 42/6, $P < 0.0001$, *Figure 3B*) and 3 Hz compared with untreated control (Iso vs. Con: F_{340}/F_{380}: 0.24 ± 0.02 vs. 0.12 ± 0.01, *n* cells/hearts = 41/6 vs. 42/6, $P < 0.0001$, *Figure 3C*). Additional neprilysin inhibition by Sac did not result in significant alterations of systolic Ca^{2+}-transient amplitude under stimulation with 1 Hz (Sac + Iso vs. Iso: F_{340}/F_{380}: 0.15 ± 0.02 vs. 0.19 ± 0.02, *n* cells/hearts = 39/6 vs. 41/6, *P* = 0.33, *Figure 3B*) and 3 Hz (Sac + Iso vs. Iso: F_{340}/F_{380}: 0.23 ± 0.02 vs. 0.24 ± 0.02, *n* cells/hearts = 39/6 vs. 41/6, *P* = 0.98, *Figure 3B*). As expected, β-adrenergic stimulation with Iso significantly increased the amplitude of caffeine-induced Ca^{2+} transients (Iso vs. Con F_{340}/F_{380}: 0.58 ± 0.10 vs. 0.29 ± 0.04, *n* cells/hearts = 15/6 vs. 19/6, *P* = 0.01, *Figure 3D*), signifying an increased SR Ca^{2+} load. Interestingly, Sac treatment did not compromise the amplitude of caffeine-induced Ca^{2+} transients (Sac + Iso vs. Iso F_{340}/F_{380}: 0.54 ± 0.06 vs. 0.58 ± 0.10, *n* cells/hearts = 18/6 vs. 15/6, *P* = 0.98, *Figure 3D*). Decay kinetics of systolic Ca^{2+} transients were significantly accelerated upon Iso treatment under stimulation with 1 Hz (Iso vs. Con: 0.27 ± 0.02 vs. 0.33 ± 0.01 s, *n* cells/hearts = 41/6 vs. 42/6, $P < 0.001$, *Figure 3E*), which was not significantly influenced by Sac treatment (*P* = 0.50, *Figure 3C*). Under 3 Hz stimulation, no effects of Iso or additional neprilysin inhibition could be detected on decay kinetics (*Figure 3F*).

To approximate SERCA activity (k_{SERCA}) as previously reported,[18] we subtracted the rate constant of decay of the caffeine-triggered transient (k_{caff}) from that of the systolic Ca^{2+} transient (k_{sys}; $k_{SERCA} = k_{sys} - k_{caff}$). Upon β-adrenergic stimulation with Iso, k_{SERCA} showed a trend towards an increased SERCA activity compared with control (Iso vs. Con: 2.08 ± 0.28 vs. 1.36 ± 0.18, *n* cells/hearts = 12/6 vs. 16/6, $P = 0.10$, *Figure 3G*). Additional treatment with Sac did not lead to significant alterations of k_{SERCA} compared with sole Iso treatment (Sac + Iso vs. Iso: 1.69 ± 0.22 vs. 2.08 ± 0.28, *n* cells/hearts = 15/6 vs. 12/6, $P = 0.60$, *Figure 3G*).

Effects of angiotensin receptor and neprilysin inhibition on sarcoplasmic reticulum Ca^{2+} leak in cardiomyocytes from human end-stage heart failure

To investigate if the results derived from murine ventricular CMs can be translated to human HF, we performed further experiments using isolated human ventricular CMs from patients with end-stage HF. Patient characteristics of myocardial samples used for these experiments are shown in *Table 1*. We, again, used confocal microscopy (Fluo-4 AM) to evaluate the effects of angiotensin receptor inhibition by Val (13 μmol/L) and neprilysin inhibition by Sac (40 μmol/L). In line with the data from murine myocardium, combined angiotensin receptor and neprilysin inhibition resulted in a significant reduction of CaSpF (Sac/Val vs. Con: 0.85 ± 0.12 vs. 1.43 ± 0.18 × 100 μm/s, *n* cells/hearts = 78/8 vs. 71/8, $P < 0.05$, *Figure 4B*) and SR Ca^{2+} leak compared with untreated control (decrease by 71 ± 6%, $P < 0.01$, *Figure 4F*). Furthermore, a reduction of Ca^{2+}-spark amplitude (F/F_0: 1.63 ± 0.02 vs. 1.73 ± 0.02, $P < 0.001$, *Figure 4C*), width (3.00 ± 0.12 vs. 3.75 ± 0.12 μm, $P < 0.001$, *Figure 4D*), and duration (36.86 ± 2.00 vs. 50.09 ± 2.53 ms, $P < 0.001$, *Figure 4E*) could be detected. Importantly, sole Sac exerted similar antiarrhythmic effects as it also yielded a reduction of CaSpF (Sac vs. Con: 0.85 ± 0.15 vs. 1.43 ± 0.18 × 100 μm/s, *n* cells/hearts = 78/8 vs. 71/8, $P < 0.05$, *Figure 4B*), Ca^{2+}-spark amplitude (F/F_0: 1.61 ± 0.02 vs. 1.73 ± 0.02, $P < 0.0001$, *Figure 4C*), width (2.99 ± 0.12 vs. 3.75 ± 0.12 μm, $P < 0.001$, *Figure 4D*), and duration (36.37 ± 1.87 vs. 50.09 ± 2.53 ms, $P < 0.001$, *Figure 4E*). This translated into a significant reduction of the calculated SR Ca^{2+} leak by 74 ± 7% upon neprilysin inhibition ($P < 0.001$, *Figure 4F*).

Effects of neprilysin inhibition on myocardial contractility of ventricular trabeculae from patients with end-stage heart failure

The impact of neprilysin inhibition on the contractility of human myocardium was evaluated in experiments with isometrically twitching ventricular trabeculae from patients with end-stage HF (1 Hz; 30 min). Patient characteristics of myocardial samples used for these experiments are shown in *Table 2*. Interestingly, no significant difference of developed force normalized to control could be detected upon Sac treatment at all respective time points over the time course of 30 min (*n* trabeculae/hearts = 3/3 vs. 4/3, *Figure 5*).

Discussion

This study investigates the functional role of angiotensin receptor and neprilysin inhibition on Ca^{2+} homeostasis and cellular arrhythmic triggers.

This study is the first to show that (i) combined angiotensin receptor and neprilysin inhibition (Val/Sac) directly decreases pro-arrhythmogenic diastolic SR Ca^{2+} leak; (ii) this potentially antiarrhythmic effect can be attributed to Sac treatment as sole Val treatment lacks respective effects on SR Ca^{2+} leak; (iii) Sac does not negatively affect systolic Ca^{2+} release as well as SR Ca^{2+} load in isolated murine CMs; (iv) these beneficial effects of Sac on SR Ca^{2+} leak equally occur in human ventricular CMs of patients with end-stage HF; and (v) myocardial contractility (developed force) of isolated isometrically twitching ventricular trabeculae from patients with end-stage HF was not compromised upon Sac treatment excluding negative inotropic effects.

Of note, Ca^{2+} is the central second messenger in cardiac excitation–contraction coupling and equally important for electric stability. Ca^{2+} ions entering the cell during an action potential via voltage-dependent L-type Ca^{2+} channels induce Ca^{2+}-induced Ca^{2+} release from the SR through cardiac ryanodine receptor type 2 and subsequently activate contractile myofilaments. Systolic Ca^{2+} release is followed by a quick Ca^{2+} reuptake into the SR by SR Ca^{2+} ATPase 2a to induce diastolic relaxation.[19] In cardiac disease, post-translational modifications of ryanodine receptor type 2 result in a distortion of diastolic closure giving rise to short and spatially limited SR Ca^{2+} release events (Ca^{2+} sparks) during diastole. An increased diastolic SR Ca^{2+} loss contributes to systolic and diastolic dysfunction through a depletion of SR Ca^{2+} stores but most of all hampers electric stability as a significant amount of Ca^{2+} is extruded from the cytosol in exchange with 3 Na^+ ions (Na^+–Ca^{2+} exchanger).[10,14,20,21] This results in a net inward current of positive charge carriers and induces delayed after-depolarizations constituting one of the main causes of triggered arrhythmias and sudden cardiac death.[22–24]

Thus, the key messages of this *in vitro* study perfectly stand in line with recent clinical data and may provide important mechanistic insights helping to explain clinical observations. The PARADIGM-HF trial showed a significant

reduction of cardiovascular death upon combined angiotensin receptor and neprilysin inhibition compared with enalapril.[5] However, the mechanisms leading to a further reduction of mortality and sudden death are not entirely clear. Whereas beneficial circulatory effects of neprilysin inhibition such as diuretic, natriuretic, and vasodilating effects as well as inhibition of RAAS and pathological growth by augmented levels of NPs are already well understood, potential direct antiarrhythmic effects on myocardial tissue are elusive.[2] Interestingly, a recent prospective study on HFrEF patients with implantable cardiac devices reported a significant decrease of ventricular arrhythmias, appropriate ICD shocks, and premature ventricular complexes upon combined angiotensin receptor and neprilysin inhibition compared with previous therapy with an angiotensin-converting enzyme inhibitor or angiotensin receptor blocker.[9] In a retrospective study on HFrEF patients with implantable cardiac devices, investigators showed a significant decrease of ventricular arrhythmias, appropriate ICD shocks, and premature ventricular complexes to a similar extent.[25] Interestingly, neither these two studies nor the PARADIGM-HF study found a significant effect of ARNI treatment on incidence of atrial fibrillation.[5,9,25] Nevertheless, these findings suggest that a reduction of ventricular arrhythmias upon ARNI treatment may also contribute to PARADIGM-HF study results. Numerous mechanisms were proposed in the literature to be responsible for the reduction of ventricular arrhythmias upon ARNI treatment: (i) anti-inflammatory, anti-fibrotic, and anti-hypertrophic effects[26–28]; (ii) modulation of the sympathetic nervous system and reduction of heart rate[25,29]; (iii) reduction of stretch-activated ventricular arrhythmias by decreased myocardial wall stress[30,31]; (iv) a higher degree of reverse remodelling[32]; (v) increased levels of enkephalins, endorphins, and bradykinin, which are also substrates of neprilysin[26]; and (vi) direct antiarrhythmic effects on CMs.[26]

Our study clearly supports the hypothesis of direct antiarrhythmic effects of Sac on myocardial tissue. We show that ARNI treatment of isolated murine WT ventricular CMs using concentrations equalling plasma concentrations of PARADIGM-HF trial patients yields a reduction of pro-arrhythmogenic SR Ca^{2+} leak under β-adrenergic stimulation (*Figure 1*). This antiarrhythmic effect can clearly be attributed to Sac treatment as sole angiotensin receptor inhibition by Val did not affect CaSpF or SR Ca^{2+} leak, whereas sole neprilysin inhibition by Sac (LBQ657) resulted in a pronounced reduction of CaSpF and SR Ca^{2+} leak (*Figure 2*).

Furthermore, we can demonstrate that neprilysin inhibition by Sac does not compromise systolic Ca^{2+} release, SERCA-related SR Ca^{2+} reuptake, and SR Ca^{2+} load (*Figure 3*). As we could confirm that neprilysin inhibition by Sac also significantly reduces pro-arrhythmogenic SR Ca^{2+} leak in human ventricular CMs from patients with end-stage HF (*Figure 4* and *Table 1*) and that this treatment does not significantly compromise inotropy (human ventricular muscle twitches, *Figure 5*), direct antiarrhythmic effects of Sac may contribute to the reduced mortality of patients receiving Sac/Val in the PARADIGM-HF trial.

These mechanistic findings are clinically important as they may influence future therapeutic developments.

Limitations

i In this study, CaSpF and calculated SR Ca^{2+} leak were classified as important and potent arrhythmic triggers. Effects of Sac on cellular and multicellular arrhythmic events could not be investigated because of a very low incidence of cellular arrhythmias in control group. However, the link between SR Ca^{2+} leak and cellular/multicellular arrhythmias has been repeatedly shown in the past.[33,34]

ii The molecular mechanism through which Sac exerts its beneficial effects on cellular Ca^{2+} homeostasis has not been elucidated in the current project. Additional measurements of cardiac action potentials and membrane currents could provide important additional information.

Conclusions

Our study shows that neprilysin inhibition by Sac (LBQ657) exerts direct antiarrhythmic effects on isolated murine and human ventricular CMs by significantly reducing pro-arrhythmogenic SR Ca^{2+} leak without acutely affecting systolic Ca^{2+} release and inotropy. Importantly, these beneficial effects may contribute to the mortality benefit of sacubitril/Val treatment reported in the pivotal PARADIGM-HF trial and therefore require further investigation.

Acknowledgements

We gratefully acknowledge the technical assistance of K.-C. Hansing and T. Schulte.

Conflict of interest

None declared.

Funding

T.H.F. is funded by the Deutsche Forschungsgemeinschaft (DFG) through the SFB 1002 (A11). S.S. is supported by the Marga und Walter Boll-Stiftung and Novartis through research grants.

References

1. Cohn JN, Tognoni G. A randomized trial of the angiotensin-receptor blocker valsartan in chronic heart failure. *N Engl J Med* 2001; **345**: 1667–1675.
2. McMurray JJV. Neprilysin inhibition to treat heart failure: a tale of science, serendipity, and second chances. *Eur J Heart Fail* 2015; **17**: 242–247.
3. O'Connor CM, Starling RC, Hernandez AF, Armstrong PW, Dickstein K, Hasselblad V, Heizer GM, Komajda M. Effect of nesiritide in patients with acute decompensated heart failure. *N Engl J Med* 2011; **365**: 32–43.
4. Jhund PS, McMurray JJV. The neprilysin pathway in heart failure: a review and guide on the use of sacubitril/valsartan. *Heart* s 2016; **102**: 1342–1347.
5. McMurray JJV, Packer M, Desai AS, Gong J, Lefkowitz MP, Rizkala AR, Rouleau JL, Shi VC, Solomon SD, Swedberg K, Zile MR. Angiotensin–neprilysin inhibition versus enalapril in heart failure. *N Engl J Med* 2014; **371**: 993–1004.
6. Ponikowski P, Voors AA, Anker SD, Bueno H, Cleland JGF, Coats AJS, Falk V, González-Juanatey JR, Harjola V-P, Jankowska EA, Jessup M, Linde C, Nihoyannopoulos P, Parissis JT, Pieske B, Riley JP, Rosano GMC, Ruilope LM, Ruschitzka F, Rutten FH, van der Meer P. 2016 ESC guidelines for the diagnosis and treatment of acute and chronic heart failure. *Eur J Heart Fail* 2016; **18**: 891–975.
7. Lohmann SM, Vaandrager AB, Smolenski A, Walter U, de Jonge HR. Distinct and specific functions of cGMP-dependent protein kinases. *Trends Biochem Sci* 1997; **22**: 307–312.
8. Kobalava Z, Kotovskaya Y, Averkov O, Pavlikova E, Moiseev V, Albrecht D, Chandra P, Ayalasomayajula S, Prescott MF, Pal P, Langenickel TH, Jordaan P, Rajman I. Pharmacodynamic and pharmacokinetic profiles of sacubitril/valsartan (LCZ696) in patients with heart failure and reduced ejection fraction. *Cardiovasc Ther* 2016; **34**: 191–198.
9. de Diego C, González-Torres L, Núñez JM, Centurión Inda R, Martin-Langerwerf DA, Sangio AD, Chochowski P, Casasnovas P, Blazquéz JC, Almendral J. Effects of angiotensin–neprilysin inhibition compared to angiotensin inhibition on ventricular arrhythmias in reduced ejection fraction patients under continuous remote monitoring of implantable defibrillator devices. *Heart Rhythm* 2018; **15**: 395–402.
10. Eiringhaus J, Herting J, Schatter F, Nikolaev VO, Sprenger J, Wang Y, Köhn M, Zabel M, El-Armouche A, Hasenfuss G, Sossalla S, Fischer TH. Protein kinase/phosphatase balance mediates the effects of increased late sodium current on ventricular calcium cycling. *Basic Res Cardiol* 2019; **114**: 13.
11. Toischer K, Hartmann N, Wagner S, Fischer TH, Herting J, Danner BC, Sag CM, Hund TJ, Mohler PJ, Belardinelli L, Hasenfuss G, Maier LS, Sossalla S. Role of late sodium current as a potential arrhythmogenic mechanism in the progression of pressure-induced heart disease. *J Mol Cell Cardiol* 2013; **61**: 111–122.
12. Fischer TH, Eiringhaus J, Dybkova N, Saadatmand A, Pabel S, Weber S, Wang Y, Köhn M, Tirilomis T, Ljubojevic S, Renner A, Gummert J, Maier LS, Hasenfuß G, El-Armouche A, Sossalla S. Activation of protein phosphatase 1 by a selective phosphatase disrupting peptide reduces sarcoplasmic reticulum Ca^{2+} leak in human heart failure. *Eur J Heart Fail* 2018; **20**: 1673–1685.
13. Fischer TH, Herting J, Eiringhaus J, Pabel S, Hartmann NH, Ellenberger D, Friedrich M, Renner A, Gummert J, Maier LS, Zabel M, Hasenfuss G, Sossalla S. Sex-dependent alterations of Ca^{2+} cycling in human cardiac hypertrophy and heart failure. *Europace* 2016; **18**: 1440–1448.
14. Fischer TH, Herting J, Tirilomis T, Renner A, Neef S, Toischer K, Ellenberger D, Förster A, Schmitto JD, Gummert J, Schöndube FA, Hasenfuss G, Maier LS, Sossalla S. Ca^{2+}/calmodulin-dependent protein kinase II and protein kinase A differentially regulate sarcoplasmic reticulum Ca^{2+} leak in human cardiac pathology. *Circulation* 2013; **128**: 970–981.
15. Gu J, Noe A, Chandra P, Al-Fayoumi S, Ligueros-Saylan M, Sarangapani R, Maahs S, Ksander G, Rigel DF, Jeng AY, Lin T-H, Zheng W, Dole WP. Pharmacokinetics and pharmacodynamics of LCZ696, a novel dual-acting angiotensin receptor–neprilysin inhibitor (ARNi). *J Clin Pharmacol* 2010; **50**: 401–414.
16. Picht E, Zima AV, Blatter LA, Bers DM. SparkMaster: automated calcium spark analysis with ImageJ. *Am J Physiol Cell Physiol* 2007; **293**: C1073–C1081.
17. Sossalla S, Wagner S, Rasenack ECL, Ruff H, Weber SL, Schöndube FA, Tirilomis T, Tenderich G, Hasenfuss G, Belardinelli L, Maier LS. Ranolazine improves diastolic dysfunction in isolated myocardium from failing human hearts —role of late sodium current and intracellular ion accumulation. *J Mol Cell Cardiol* 2008; **45**: 32–43.
18. Bode EF, Briston SJ, Overend CL, O'Neill SC, Trafford AW, Eisner DA. Changes of SERCA activity have only modest effects on sarcoplasmic reticulum Ca^{2+} content in rat ventricular myocytes. *J Physiol* Wiley-Blackwell 2011; **589**: 4723–4729.
19. Fischer TH, Maier LS, Sossalla S. The ryanodine receptor leak: how a tattered receptor plunges the failing heart into crisis. *Heart Fail Rev* 2013: 475–483.
20. Belevych AE, Radwański PB, Carnes CA, Györke S. 'Ryanopathy': causes and manifestations of RyR2 dysfunction in heart failure. *Cardiovasc Res* 2013; **98**: 240–247.
21. Dobrev D, Wehrens XHT. Role of RyR2 phosphorylation in heart failure and arrhythmias: controversies around ryanodine receptor phosphorylation in cardiac disease. *Circ Res* 2014; **114**: 1311–1319.
22. Xie Y, Yang Y, Galice S, Bers DM, Sato D. Size matters: ryanodine receptor cluster size heterogeneity potentiates calcium waves. *Biophys J* 2019; **116**: 530–539.
23. Keizer J, Smith GD, Ponce-Dawson S, Pearson JE. Saltatory propagation of Ca^{2+} waves by Ca^{2+} sparks. *Biophys J* 1998; **75**: 595–600.
24. Belevych AE, Ho H-T, Bonilla IM, Terentyeva R, Schober KE, Terentyev D, Carnes CA, Györke S. The role of spatial organization of Ca^{2+} release sites in the generation of arrhythmogenic diastolic Ca^{2+} release in myocytes from failing hearts. *Basic Res Cardiol* 2017; **112**: 44.
25. Martens P, Nuyens D, Rivero-Ayerza M, van Herendael H, Vercammen J, Ceyssens W, Luwel E, Dupont M, Mullens W. Sacubitril/valsartan reduces ventricular arrhythmias in parallel with left ventricular reverse remodeling in heart failure with reduced ejection fraction. *Clin Res Cardiol* 2019; **108**: 1074–1082.
26. Sarrias A, Bayes-Genis A. Is sacubitril/valsartan (also) an

antiarrhythmic drug? *Circulation* 2018; **138**: 551–553.
27. Vicent L, Juárez M, Bruña V, Devesa C, Sousa-Casasnovas I, Fernández-Avilés F, Martinez-Sellés M. Clinical profile and ventricular arrhythmias after sacubitril/valsartan initiation. *Cardiology* 2019; **142**: 26–27.
28. Hubers SA, Brown NJ. Combined angiotensin receptor antagonism and neprilysin inhibition. *Circulation* Lippincott Williams and Wilkins 2016; **133**: 1115–1124.
29. Chin KL, Collier T, Pocock S, Pitt B, McMurray JJV, van Veldhuisen DJ, Swedberg K, Vincent J, Zannad F, Liew D. Impact of eplerenone on major cardiovascular outcomes in patients with systolic heart failure according to baseline heart rate. *Clin Res Cardiol* Dr. Dietrich Steinkopff Verlag GmbH and Co. KG 2019; **108**: 806–814.
30. Levine YC, Rosenberg MA, Mittleman M, Samuel M, Methachittiphan N, Link M, Josephson ME, Buxton AE. B-type natriuretic peptide is a major predictor of ventricular tachyarrhythmias. *Heart Rhythm* Elsevier 2014; **11**: 1109–1116.
31. Alter P, Rupp H, Rominger MB, Vollrath A, Czerny F, Klose KJ, Maisch B. Relation of B-type natriuretic peptide to left ventricular wall stress as assessed by cardiac magnetic resonance imaging in patients with dilated cardiomyopathy. *Can J Physiol Pharmacol* 2007; **85**: 790–799.
32. Martens P, Beliën H, Dupont M, Vandervoort P, Mullens W. The reverse remodeling response to sacubitril/valsartan therapy in heart failure with reduced ejection fraction. *Cardiovasc Ther* 2018; **36**: e12435.
33. Sag CM, Mallwitz A, Wagner S, Hartmann N, Schotola H, Fischer TH, Ungeheuer N, Herting J, Shah AM, Maier LS, Sossalla S, Unsöld B. Enhanced late I_{Na} induces proarrhythmogenic SR Ca leak in a CaMKII-dependent manner. *J Mol Cell Cardiol* 2014; **76**: 94–105.
34. Fischer TH, Eiringhaus J, Dybkova N, Förster A, Herting J, Kleinwächter A, Ljubojevic S, Schmitto JD, Streckfuß-Bömeke K, Renner A, Gummert J, Hasenfuss G, Maier LS, Sossalla S. Ca^{2+}/calmodulin-dependent protein kinase II equally induces sarcoplasmic reticulum Ca^{2+} leak in human ischaemic and dilated cardiomyopathy. *Eur J Heart Fail* 2014; **16**: 1292–1300.